Title

Direct imaging of interactions between an icosahedral virus and conjugate F(ab) fragments by cryoelectron microscopy and X-ray crystallography.

Journal

Virology, 204(2)

ISSN

0042-6822

Authors

Porta, C
Wang, G
Cheng, H
et al.

Publication Date

1994-11-01

DOI

10.1006/viro.1994.1593

Peer reviewed

VIROLOGY 204, 777–788 (1994)

Direct Imaging of Interactions between an Icosahedral Virus and Conjugate F_{ab} Fragments by Cryoelectron Microscopy and X-Ray Crystallography

CLAUDINE PORTA,[1,2] GUOJI WANG,[1,3] HOLLAND CHENG, ZHONGGUO CHEN,[4] TIMOTHY S. BAKER, AND JOHN E. JOHNSON[5]

Department of Biological Sciences, Purdue University, West Lafayette, Indiana 47907-1392

Received April 21, 1994; accepted July 14, 1994

The binding properties of seven mouse monoclonal antibodies (McAbs) raised against cowpea mosaic virus (CPMV) were characterized by conventional and inhibition enzyme-linked immunosorbent assay (ELISA) technique. McAb binding to CPMV on electron microscope (EM) grids was also assayed with gold-labeled anti-mouse antibodies. Two of the seven McAbs (5B2 and 10B7) were found to bind tighter to CPMV than the others in the inhibition ELISA and the EM assay. F_{ab} fragments from both of these McAbs were prepared and complexed with CPMV in solution. Electron micrographs of flash frozen (vitrified) samples of native CPMV and CPMV complexed with F_{ab} fragments from McAbs 5B2 and 10B7 as well as IgGs from 5B2 were recorded and reconstructions were computed at 23 Å resolution for the CPMV/F_{ab} complexes and 30 Å resolution for the CPMV/IgG complex. Structures of all three complexes clearly displayed the F_{ab} fragments distributed with icosahedral symmetry on the surface of CPMV. The IgG bound in a monodentate fashion with only one F_{ab} attached to the virus surface. F_{ab} fragments from 5B2 and 10B7 bound to nearly identical positions. The refined 2.8 Å X-ray structure of CPMV was used to identify the roughly 30 amino acids covered by the F_{ab} fragments. The "footprint" spans a subunit interface and appears spatially similar to antigenic site 3B on poliovirus. In a previous, preliminary report of the CPMV/F_{ab} 5B2 complex (Wang *et al.*, 1992, *Nature* 355, 275–278) the wrong enantiomorph of the reconstruction was chosen. This was corrected and, since the F_{ab} binds close to a mirror plane, the change in the footprint was minor.

INTRODUCTION

Immune recognition and neutralization of viral antigens are problems of fundamental and practical importance. The antigenic surfaces of the influenza virus hemagglutinin and a variety of picornaviruses have been extensively mapped by three methods: (i) analysis of naturally occurring mutants that result in outbreaks of disease (e.g., Wiley *et al.*, 1981), (ii) analysis of binding of monoclonal antibodies generated by immunization with polypeptides corresponding to contiguous amino acid sequences in the viral protein (e.g., Attassi and Kurisaki, 1984; Chow *et al.*, 1985), and (iii) analysis of changes in envelope or coat protein sequences found in viral variants that avoid neutralization by particular monoclonal antibodies (e.g., Rossmann *et al.*, 1985; Sherry *et al.*, 1986; Page *et al.*, 1988). The data derived from these studies correlate well with the known three-dimensional structures of the influenza virus hemagglutinin (Wilson and Cox, 1990) and a number of picornaviruses (Rossmann *et al.*, 1985; Hogle *et al.*, 1985; Page *et al.*, 1988). Until recently the biochemical and structural data for icosahedral viruses could only be obtained in independent experiments, making it impossible to directly establish the mode of interaction between the viral immunogenic site and the antibody, although reasonable models were developed on the basis of high resolution X-ray studies of F_{ab} fragments complexed with protein antigens (Amit *et al.*, 1986; Padlan *et al.*, 1989; Colman *et al.*, 1987).

We recently reported the moderate resolution structure of an icosahedral virus, cowpea mosaic virus (CPMV), complexed with a F_{ab} fragment that was derived from a monoclonal antibody (McAb) to the virus, designated 5B2 (Wang *et al.*, 1992). We now present the procedures used for the production and structure determination of the CPMV/F_{ab} 5B2 complex and report the study of CPMV complexed to a F_{ab} fragment derived from a different monoclonal antibody, called 10B7. In the course of extending this investigation we employed a new technique for computing the reconstructions and we discovered that we had chosen the wrong enantiomorph in the original report of the CPMV complex with 5B2. Since the site of binding is close to a mirror plane, the revision of the

[1] Co-First Authors

[2] Present address: John Innes Centre, Colney Lane, Norwich NR4 7UH, England.

[3] Present address: University of Pittsburgh School of Medicine, Department of Pathology, Scaife Hall Room S-790, Pittsburgh, PA 15261.

[4] Present address: Merck Sharp & Dohme Research Laboratories, Division of Merck & Co., Inc., West Point, PA 19486.

[5] To whom correspondence and reprint requests should be addressed.

0042-6822/94 $6.00

footprint in the light of this discovery was minor. The F_{ab} fragment of McAb 10B7 covers nearly the same region of the viral surface as 5B2. We also report the structure of the IgG of monoclonal antibody 5B2 complexed to the virus and show that it binds in a monovalent fashion, i.e., with only one of the two F_{ab} portions attached to the surface.

CPMV is a multicomponent, single-stranded, RNA plant virus (for a recent review see Lomonossoff and Johnson, 1991). Typical preparations are composed of empty capsids (called top component or CPMV-T), capsids which contain the 3481-base RNA2 (called middle component or CPMV-M), and capsids which contain the 5889-base RNA1 (called bottom component or CPMV-B). The external surfaces of the three different particles are virtually identical because they cocrystallize in a single crystal that diffracts X rays to 2.8 Å resolution (White and Johnson, 1980).

The CPMV capsid has an architecture similar to that of the picornaviruses with the icosahedral asymmetric unit formed by three β-barrel structures where each β-barrel has a unique sequence, but all three have strikingly similar tertiary structures (Chen *et al.*, 1989; 1990). Two of the β-barrels are part of a single polypeptide chain (42 kDa) corresponding to the "large" (L) capsid protein. The β-barrel of the L protein, analogous to VP2 of picornaviruses, is at the amino end of the polypeptide, and the β-barrel corresponding to VP3 of picornaviruses is at the carboxy end of the chain. These two β-barrels, along with the corresponding β-barrels from two neighboring L proteins, form a pseudo hexamer about the icosahedral threefold symmetry axes. The third β-barrel is analogous to VP1 of picornaviruses; it is a single polypeptide chain (23 kDa), called the "small" (S) capsid protein, and forms the pentamers at the 12 particle vertices. Like picornaviruses, the CPMV capsid proteins are initially synthesized as a polyprotein that is processed by a virally encoded protease.

The structures of native CPMV and the CPMV/F_{ab} 5B2 complex, determined by cryoelectron microscopy (cryo-EM) and image reconstruction, were compared with the refined 2.8 Å structure of native CPMV determined by X-ray crystallography (Chen *et al.*, 1990). A detailed footprint of the F_{ab} (identification of all amino acids covered by the F_{ab}) on the viral surface was determined and this was found to correlate (with respect to the quaternary particle structure) with an antigenic site on poliovirus 1, known as 3B. Site 3B was identified by the analysis of escape mutations (Page *et al.*, 1988) and has been further explored by site-directed mutagenesis (Reynolds *et al.*, 1991). The common immunogenic sites on CPMV and poliovirus probably arise because of the overall similarity in the capsids of the two viruses which is illustrated in Fig. 1.

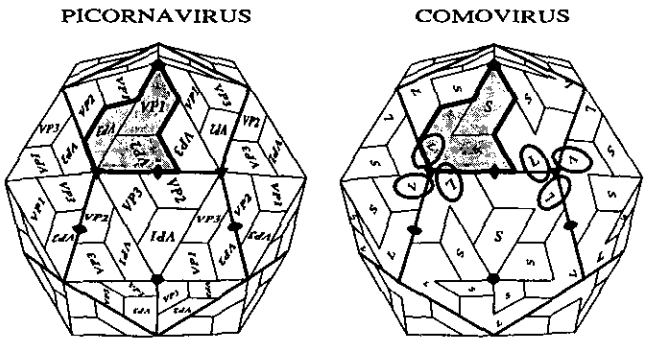

FIG. 1. A comparison of the picorna and comovirus capsids with 6 (of the 60) F_{ab} footprints on the comovirus capsid represented by ellipsoids. The picornavirus particle is formed from 60 copies each of three different, but similar, gene products (each composed of an eight-stranded, antiparallel β-barrel) labeled VP1, VP2, and VP3. The comovirus capsid is formed of 60 copies each of a large (L) subunit and a small (S) subunit. The L subunit is formed of two β-barrels corresponding to VP2 at the amino end and VP3 at the carboxy end while S corresponds to VP1. Note that the footprint spans a subunit interface with the smaller part of it interacting with the VP2 portion of one L subunit and the larger part of it interacting with the VP3 portion of a different L subunit.

MATERIALS AND METHODS

Production of monoclonal antibodies

Immunizations. Monoclonal antibodies to CPMV were generated in two separate fusion experiments. Three Balb/c mice were injected three times with 50 μg of CPMV in the first fusion experiment. The first two injections were given intraperitoneally at an interval of 10 days, the third injection was given, intramuscularly, 3 weeks later. In the second fusion experiment Balb/c mice were immunized twice subcutaneously, first with 100 μg and then with 50 μg of virus and then twice with intramuscular injections of 25 μg of virus each. The four immunizations were spaced by 8 days. Booster injections were performed after a period of rest of 1 and 2 months, respectively, for the first and the second fusion. These intravenous injections with 10 μg of virus were administered to the mice presenting the highest specific antibody serum titer, 4 and 3 days before sacrificing the animals. For the intraperitoneal and subcutaneous injections, the antigen was emulsified in an equal volume of Freund's complete adjuvant, while Freund's incomplete adjuvant was used for the intramuscular immunizations.

Hybridoma preparation. A protocol adapted from Fazekas de St. Groth and Scheidegger (1980) was used to carry out the fusion procedures. Spleen lymphocytes were fused in a 1/1 ratio with PAI myeloma cells (Stocker *et al.*, 1982) in the presence of 50% sterile filtered polyethylene glycol 4000. Hybridoma cells were grown in RPMI-based medium and selected by the presence of HAT (hypoxanthine, aminopterine, thymidine). Subcloning of hybridomas that secreted CPMV-specific antibody was

performed by a limiting dilution method in which an average of 0.5 cell per well is distributed on tissue culture plates. The McAbs were amplified in ascites fluid induced in pristane-primed Balb/c mice by injecting 0.5×10^7 cells of subcloned hybridomas into the peritoneal cavity.

Screening test

Detection of the hybridoma clones that secreted antibodies specific for CPMV was performed by ELISA. Two types of assays were used. In the DAS (double antibody sandwich)–ELISA (enzyme-linked immunosorbent assay) format, rabbit antibodies raised against CPMV were adsorbed at a concentration of 1 μg/ml in 0.05 *M* carbonate buffer, pH 9.6 (coating buffer), to the polyvinyl microtiter plates (Falcon 3912, Beckton Dickinson). Adsorption was for 3 hr at 37°. Incubation of CPMV at 1 μg/ml in PBS-T (PBS containing 0.05% Tween 20) followed for 2 hr at 37°. In ACP (antigen-coated plate)–ELISA the plates were coated with 2 μg/ml of CPMV in coating buffer for 3 hr at 37°. In both assay procedures, the subsequent steps were identical. First the remaining binding sites on the plastic were saturated by incubation with 1% BSA in PBS-T overnight at 4°. Hybridoma culture supernatants diluted 1/3 in PBS-T were then added to the wells for 2 hr at 37°. Bound McAbs were detected with a sheep anti-mouse IgG alkaline phosphatase conjugate (Jackson Laboratories, West Grove) diluted 1/1000 in PBS-T, followed by addition of the substrate *p*-nitrophenyl phosphate at 1 mg/ml in 0.1 *M* diethanolamine, pH 9.8 (substrate buffer). Each incubation step on the microtiter plates was followed by three washes with PBS-T. The isotype of McAbs from hybridoma supernatants was determined in indirect ELISA with subclass specific rabbit anti-mouse antisera (Nordic, Tilburg) and a goat anti-rabbit IgG alkaline phosphatase conjugate (Sigma Chemical Co.). For these experiments, chicken antibodies directed against CPMV were used as the first antibody in DAS–ELISA.

Purification of IgGs from ascites fluids

The protocol described by McKinney and Parkinson (1987) was followed. The ascites fluids were treated with caprylic acid to precipitate the albumin and non-IgG proteins and then with ammonium sulfate to precipitate the IgG fraction.

Production of F_{ab}s

A method employing papain attached to beaded agarose (Sigma Chemical Co.) and adapted from that described by Coulter and Harris (1983) was used. Purified IgGs were dialyzed against TNE (50 m*M* Tris, 150 m*M* NaCl, 2 m*M* EDTA, pH 7.5) and a suspension of papain–agarose in TNE was prepared. Dithiothreitol, 10 m*M* final, was added to the IgG solution and the resuspended papain 5 min before mixing of the two reagents followed by incubation at 37° under continuous shaking. Ten units of papain were used to digest 10 mg of IgG and the optimal length of incubation was determined by a kinetic study of the digestion of a small sample of McAb. The insoluble enzyme was subsequently pelleted at 2000 *g* for 5 min and the digestion products were dialyzed against PBS. The dialysate was either used as a F_{ab} fragments and Fc regions mix or purified further.

Purification of F_{ab} fragments

The papain digestion products were purified on a protein G-column (Pierce Chemical Co.), used according to the manufacturer's instructions. Protein G binds the Fc regions of immunoglobulins (Akerström and Björck, 1986) which were therefore retained on the column in binding buffer (0.1 *M* sodium acetate, pH 5.0) while the F_{ab} fragments were collected in the flow through and subsequently dialyzed against PBS and concentrated on Centricon 10,000 (Millipore Corp.). Regeneration of the protein G column was with elution buffer (0.1 *M* glycine–HCl, pH 2.8).

Immunogold labeling method

Five microliters of virus particles at 1 mg/ml in PBS was adsorbed directly on the surface of carbon-coated, formvar grids for 1 min. After saturation of the carbon surface with 1% BSA in PBS for 20 min, 5 μl of McAb, as a purified IgG or an ascites fluid, diluted in PBS was incubated for 15 min. Binding of the McAb was revealed by incubation for 15 min with 5 μl of goat anti-mouse immunoglobulins conjugated to gold particles (Sigma Chemical Co.) and diluted 1/20 in PBS. Grids were stained with 1% uranyl acetate for 1 min. Three washes with PBS were performed between each incubation step.

Inhibition ELISA

Rabbit anti-CPMV IgGs were adsorbed to ELISA plates at a concentration of 1 μg/ml in coating buffer for 3 hr at 37°. After a 1 hr saturation step with 1% powdered milk in PBS-T, 2 μg/ml of CPMV-M in PBS-T was incubated for 2 hr. During this interval, the McAbs were preincubated with concentrations of free CPMV-M ranging from 125 to 0.25 μg/ml in PBS-T. The virus–antibody solutions were subsequently incubated on the plates for 2 hr at 37°. Immobilized McAbs were detected with sheep anti-mouse immunoglobulins conjugated to alkaline phosphatase and diluted 1/5000 in PBS-T, followed after 2 hr by *p*-nitrophenyl phosphate at 1 mg/ml in substrate buffer. Between every step of incubation the microtiter plates were washed three times with PBS-T.

Production of virus–F_{ab} complexes for cryoelectron microscopy

CPMV-M (100 μg) and F_{ab} fragments from McAb 5B2 were incubated in a ratio of 1:600 in 500 μl of PBS for 2 hr at 37°. Unbound antibody fragments were separated from virus–F_{ab} complexes by centrifugation on a 5–40% linear sucrose gradient for 2 hr at 38,000 rpm. Peaks obtained with an ISCO density gradient fractionator were screened by EM of negatively stained samples. Gradient fractions containing virus particles saturated with F_{ab} fragments were identified and subjected to centrifugation through Ultrafree-MC filters of MW cut off 100,000 (Millipore Corp.) to remove the sucrose.

CPMV-M at a concentration of 0.2 mg/ml was incubated with purified F_{ab} fragments from McAb 10B7 in a molar ratio of 1:120 in a volume of 20 μl PBS, for 5 min at 37°. The reaction volume was then brought to 400 μl with PBS and EM grade I glutaraldehyde (Sigma Chemical Co.) was added to a final concentration of 0.1%. The incubation was continued for 10 min at room temperature, before concentration and washing of the sample with PBS on Ultrafree-MC filters (MW cut off 100,000).

Production of virus–IgG complexes

CPMV (100 μg) was incubated with IgGs from McAb 5B2 in a final volume of 200 μl. A 1:60 ratio of virus to antibody was chosen in order to minimize virus particle aggregation and the level of background due to unbound antibody. Freezing of the samples for cryoEM followed within minutes after mixing the two reagents.

Cryoelectron microscopy and image reconstruction

The cryoEM and image analysis procedures that were used to obtain the three-dimensional reconstructions of CPMV and the CPMV/F_{ab} complexes were essentially similar to those previously reported (Baker *et al.*, 1991; Cheng *et al.*, 1992; Dryden *et al.*, 1993). The sample was maintained at near liquid nitrogen temperature in a Gatan 626 cryotransfer stage (Gatan, Inc., Warrendale, PA) in a Phillips EM420 transmission electron microscope (Phillips Electronics Instruments, Mahwah, NJ). Micrographs were recorded under minimal dose conditions ($<20e^-/Å^2$) at an objective lens defocus of ~0.8 μm and an instrument magnification setting of ×49,000. Micrograph selection and digitization and particle image selection were performed as previously described (Baker *et al.*, 1991; Cheng *et al.*, 1992; Dryden *et al.*, 1993).

Cross-common lines procedures (Fuller, 1987; Baker *et al.*, 1988) were used to select out a set of particle images from which the final three-dimensional reconstructions, with full 532 icosahedral symmetry (Fuller, 1987) were computed. An *R*-factor calculation (Winkelmann *et al.*, 1991) indicated that the data were reliable to ~23 Å for the CPMV/F_{ab} complexes and 30 Å resolution for the CPMV/IgG complex. Each of these resolution values was estimated on the basis of a comparison (e.g., Baker *et al.*, 1991; Dryden *et al.*, 1993) between two separate reconstructions that were computed from smaller and independently refined subsets of images.

X-ray crystallography

CPMV crystallizes in space group I23 (a = 317 Å) with two molecules in the cell. Only the fivefold symmetry axes of the particle are noncrystallographic since the particles are positioned on tetrahedral (23) symmetry sites of the crystal lattice. The CPMV structure was solved by multiple isomorphous replacement and phase refinement by real space averaging. A detailed model was constructed to fit the electron density and this model was refined with the programs PROLSQ (Hendrickson, 1985) and X-PLOR (Brunger, 1988). The final structure had a crystallographic agreement factor for all data with $I/\sigma(I) > 4$ between 6.0 and 2.8 Å of 18.1% with an rms bond distance deviation of 0.019 Å. The final model included 4510 protein atoms and 84 water molecules in the icosahedral asymmetric unit (unpublished data).

RESULTS

Production and characterization of monoclonal antibodies

Mice immunizations and the initial screening of cell culture supernatants were done with unfractionated CPMV (a mixture of top, middle, and bottom components). Subclonings were performed with CPMV-M as the test antigen in ELISA. CPMV-M was used in all the experiments described hereafter.

Ten stable hybridomas were obtained. Eight of the clones (1A1, 5B2, 8C8, 9B2, 10B7, 15A4, 29E4, and 32F5) originated from the first fusion experiment and secreted McAbs of the IgG2a isotype. The second fusion experiment produced only two clones, secreting, respectively, an IgG1 (IVB6) and an IgM (VID7). With the exception of VID7 which could only be cultured *in vitro*, specific ascites were produced in Balb/c mice for all the clones.

Nine McAbs reacted with CPMV in DAS–ELISA; however, only McAb VID7 was able to recognize CPMV coated directly to the plastic in ACP–ELISA. Since direct binding to the plate is assumed to result in partial denaturation of the virus particles (McCullough *et al.*, 1985) all the McAbs but VID7 must be sensitive to the quaternary structure of the CPMV particle. McAbs IVB6 and 8C8 could only be produced in small amounts in ascites fluids and were not considered further in this study. The reactivities of the seven McAbs for which several milligrams of IgG could be purified from ascites fluid were examined

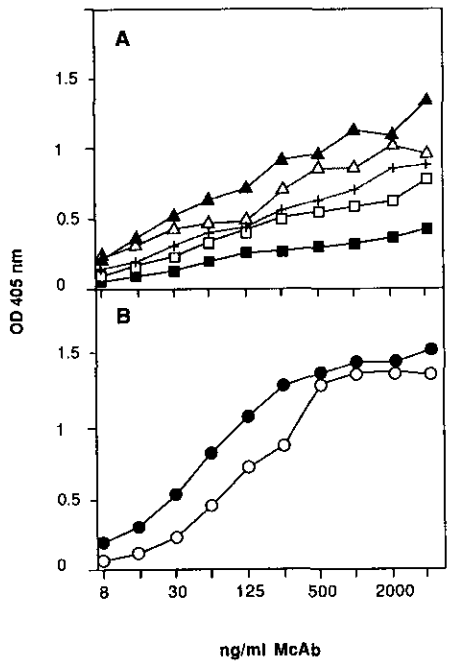

FIG. 2. Reactivity in DAS–ELISA of (A) McAbs 1A1 (■), 9B2 (□), 15A4 (▲), 29E4 (△), 32F5 (+) and (B) McAbs 5B2 (●), 10B7 (○) with CPMV-M. Plates were coated with rabbit anti-CPMV IgGs at 2 μg/ml in coating buffer and saturated with 1% milk in PBS-T. CPMV-M was incubated at 1 μg/ml in PBS-T. The bound McAbs were detected with a sheep anti-mouse IgG enzyme conjugate diluted 1/5000 in PBS-T. Substrate hydrolysis time was 90 min in A and 15 min in B.

(Fig. 2). They can be classified into two categories: the strong binding IgGs 5B2 and 10B7 (Fig. 2B) and the moderate binders 1A1, 9B2, 15A4, 29E4, and 32F5 (Fig. 2A) of which some reach OD 405-nm readings of the same order of magnitude as the antibodies in Fig. 2B, but after a much longer enzyme substrate incubation time. Since identical concentrations of the different IgGs were used, the relative absorbances can be correlated with binding affinity.

To initiate the investigation of virus–antibody complexes by EM, conditions were sought in which antibody binding to virus in the solid phase could be readily monitored. An immunogold labeling assay was developed in which the binding of McAbs to virus, directly adsorbed to the EM grids, was revealed by an anti-mouse antisera conjugated to gold particles. Of the seven McAbs studied, only two, 5B2 and 10B7, were positive in this binding assay (Fig. 3).

Although there is some similarity between the ACP–ELISA and the immunogold labeling technique, insofar as both assays involve virus particles directly adsorbed to a solid phase, McAbs 5B2 and 10B7 gave a clear positive result in the immunogold analysis and a negative result in the ACP–ELISA. The most likely explanation is the difference in the conditions for adsorption. In the EM assay the virus is adsorbed to the carbon-coated formvar grids in PBS at pH 7.4, whereas coating to the plastic surface of a microtiter plate requires a pH 9.6 buffer. The latter conditions at least partially denature the virus particles and alter their antigenic properties (Dore *et al.*, 1988).

The binding of monoclonal IgG molecules to CPMV was also monitored by an assay in solution. The screening for tight-binding McAbs was carried out in a DAS–ELISA by reacting a McAb with soluble virus prior to incubation in microtiter plates where virus particles were immobilized. The trapping of specific IgGs by virus particles in solution results in a decrease in the amount of antibody available for interaction with the solid-phase virus particles. Six of the McAbs were assayed for their ability to bind to soluble CPMV-M in this inhibition ELISA.

Binding to solid-phase CPMV-M of McAb 10B7 (Fig. 4), as well as McAb 5B2 (result not shown) was already significantly inhibited by less than 1 μg/ml of soluble CPMV-M while a concentration range of 10 to 100 μg/ml of soluble virus was necessary to affect the binding of IgGs 9B2 and 29E4. McAbs 1A1 and 15A4 had behaviors intermediate between those of 9B2 and 29E4 (results not shown).

Solution complex formation of CPMV with F_{ab}s 5B2 and 10B7

The solid- and solution-phase binding assays clearly differentiate 5B2 and 10B7 as exceptionally tight-binding antibodies when compared with the seven other monoclonal antibodies examined. Monoclonal antibodies 5B2 and 10B7 were therefore chosen to study the interaction of antibodies with native virus particles. Initial attempts to complex IgG molecules of these clones with virus in solution resulted in the formation of aggregates. This problem could be only partially circumvented by variation of the concentrations and ratios of the interacting molecules. The assays for aggregation were monitored by both EM and light scattering (results not shown). Since the aggregated particles in most micrographs were unsuitable for image reconstruction, monovalent binding F_{ab} fragments were prepared by papain cleavage of the immunoglobulin chains. Complexes of F_{ab}s derived from 5B2 and 10B7 were formed with CPMV-M at different molar ratios in solution. The F_{ab} 5B2 and CPMV reaction mix was centrifuged on a sucrose gradient. Fractionation of the gradient allowed resolution of two separate peaks, the unbound F_{ab} fragments, which remained at the top of the gradient, and the virus–F_{ab} complexes (Fig. 5).

Analysis of the fractions within the virus–F_{ab} peak showed a variation in the number of F_{ab} fragments attached to the virus, with the slowest sedimenting portion of the peak containing the greatest number of attached F_{ab} fragments. (Although the complex has a greater molecular weight, the increased size of the com-

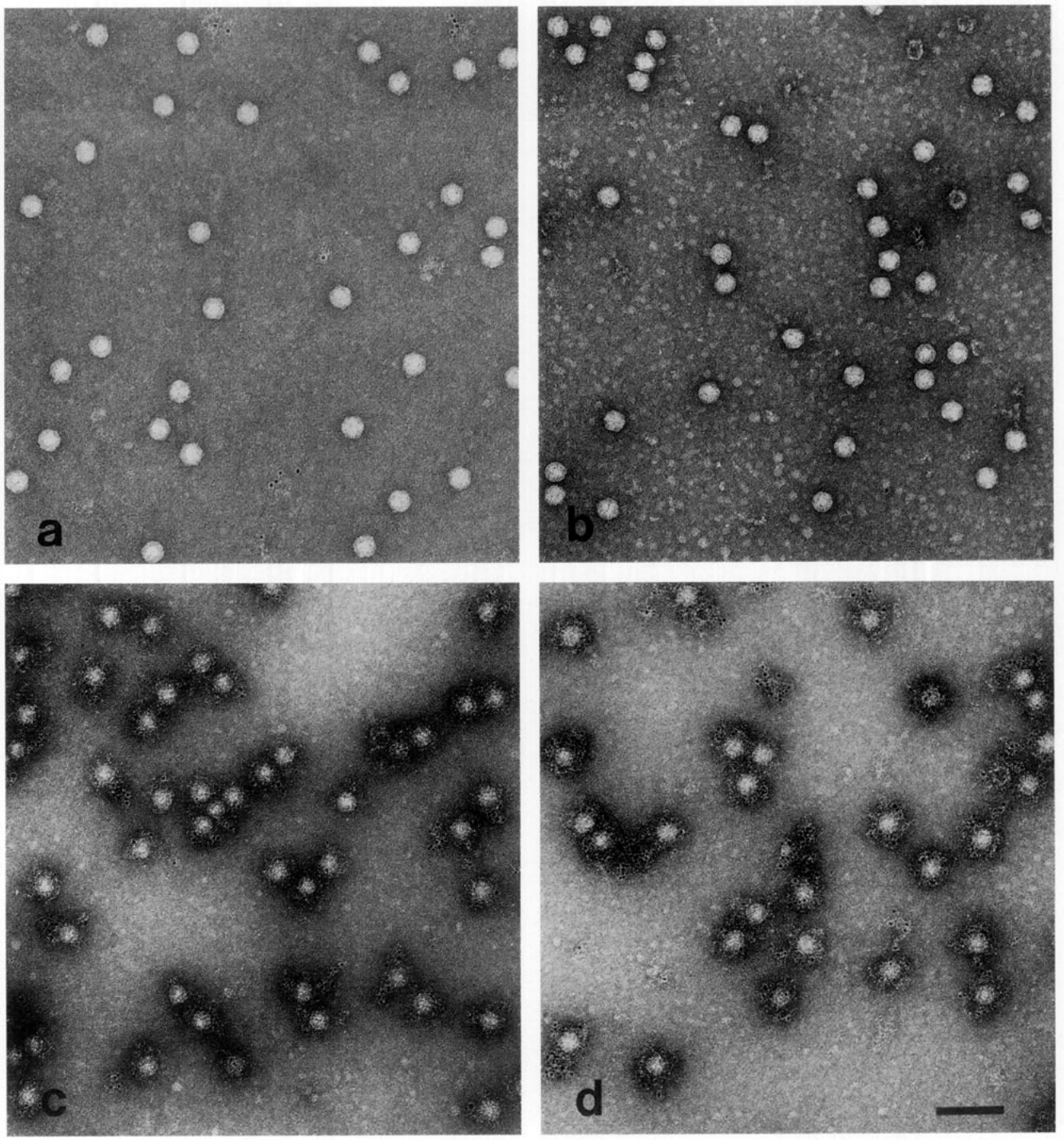

FIG. 3. Electron micrographs of negatively stained samples illustrating the variation in binding of different monoclonal antibodies to CPMV. (a) Native CPMV particles stained with 1% uranyl acetate. (b) The EM binding assay with McAb 29E4 illustrating a typical negative result with this protocol. (c) The EM binding assay applied to McAb 5B2. (d) The EM binding assay applied to McAb 10B7. Only McAb 5B2 (c) and McAb 10B7 (d) gave positive results with this assay and these were used for the studies performed with cryoEM. The bar corresponds to 100 nm.

plex actually reduces the *S* value.) The sucrose had to be removed from the fractions by ultrafiltration to allow rapid vitrification of the samples (Trinick and Cooper, 1990).

It was more difficult to produce homogeneous F_{ab}–virus complexes with McAb 10B7. Low speed centrifugation over the ultrafiltration device resulted in significant losses of F_{ab} fragments from the virus surface. Incubation of the virus with purified F_{ab} fragments (Fc regions removed by adsorption to protein G) without any further

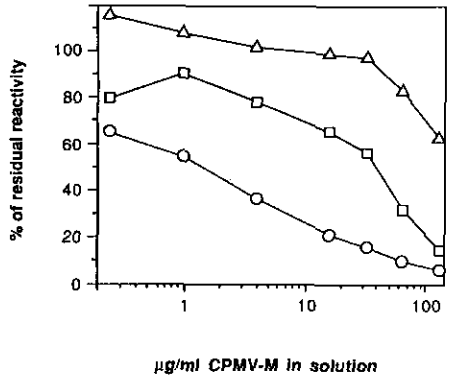

FIG. 4. Inhibition of the binding of several McAbs to solid-phase CPMV by preincubation with soluble CPMV is monitored in this DAS–ELISA experiment. CPMV-M (2 µg/ml) was used to saturate the rabbit anti-CPMV coating IgGs adsorbed at 1 µg/ml. McAbs 29E4 (△) and 9B2 (□) were used as IgG preparations at a final concentration of 0.5 µg/ml while ascites fluid 10B7 (○) was diluted 10^{-6}. Substrate incubation was for 2 hr. Results are expressed as the percentage of reactivity of each McAb relative to the control experiment in which the McAb was not preincubated in the presence of soluble CPMV-M.

treatment resulted in high background levels of unbound F_{ab} fragments. A stable complex was formed with an alternative approach in which purified 10B7 F_{ab} fragments were incubated with CPMV-M in a small volume. The addition of a dilute solution of glutaraldehyde (after reducing the concentration of the complex to prevent virus particle aggregation) allowed a limited crosslinking of the F_{ab} fragments to the viral coat proteins which reduced F_{ab} shedding during the subsequent ultrafiltration-concentration over a 100,000 MW cut off filter. This step was required to produce a sufficient concentration of virus particles complexed with F_{ab} fragments (0.5 mg/ml minimum) for the preparation of frozen-hydrated samples.

Cryoelectron microscopy of CPMV complexed with F_{ab} of 5B2 and 10B7 and IgG of 5B2

CryoEM images were recorded for native CPMV and each of the complexes (Fig. 6). The complex with IgG had a distinctly different appearance from those with F_{ab} with significant numbers of particles crosslinked and regions of density extending further from the viral surface than observed with the F_{ab} complexes. Stereoviews of the image reconstructions of native CPMV, and of the complexes of CPMV with F_{ab} fragments from monoclonal antibodies 5B2 and 10B7 and the IgGs of 5B2 reveal the overall morphologies of these structures (Fig. 7). The two F_{ab} complexes are nearly indistinguishable, yet the two monoclonal antibodies are different in their behavior in solution and when digested with papain, eliminating any possibility that they are the same. The appearance of the IgG complex shows that the binding is monodendate. The Fc portion of the IgG and the F_{ab} fragment that is not attached to the viral surface have sufficient mobility that they are only marginally detected in the reconstruction. In addition to the density of the bound F_{ab}, in the virus–IgG (5B2) reconstruction there are two regions of density that are clearly above background, but appear as "islands" of density which are not visibly attached to the virus surface or the F_{ab} that is in contact with the virus surface. One of these regions suggests the approximate average position of the unbound F_{ab} of the IgG. The mobility of the Fc fragment makes assignment of density for this portion of the IgG more speculative. A molecular model of F_{ab} (Kol) and the refined structure of CPMV were fit into the electron density of the image reconstruction of CPMV/F_{ab} 10B7 (Figs. 8 and 9, respectively). Such modeling allowed the footprint of the F_{ab}s to be accurately defined on the CPMV surface and thereby identified residues that are likely to be involved in the interaction with the antibody. Lys34 (VP2 domain) and Thr25 (VP3 domain) are particularly prominent within this F_{ab} footprint. These residues are located on the outermost loops of the VP2 and VP3 domains, respectively. The footprints of the F_{ab} and IgG of 5B2 and the F_{ab} of 10B7 are nearly identical, indicating that there is no difference in binding of the IgG and the F_{ab} of 5B2 and also that 10B7 binds to virtually the same site as 5B2.

Although the F_{ab} (Kol) model fits the density quite well, it is impossible to a priori determine unambiguously its orientation, in terms of the respective positions of the heavy and light immunoglobulin chains. Either of two orientations that are related by a 180° rotation about the pseudo dyad axis that relates light and heavy chains, fit the density equally well. The F_{ab} extends radially from the surface of the virus about 70 Å and the shape of the density indicates that the elbow angle is nearly linear, i.e., 180°, (Fig. 8). The footprint (shown in Fig. 9) has an ellipsoidal boundary with major and minor axes of 40 and 20 Å. The approximate center of the footprint is located 25 Å from the icosahedral threefold axes. Roughly 30 residues lie entirely under the footprint of the F_{ab} and 6

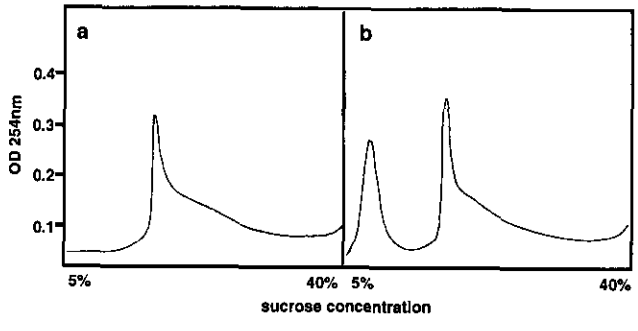

FIG. 5. Sucrose gradient density profiles of CPMV-M alone (a) and complexed to 5B2 F_{ab} fragments in a ratio of 1 to 600 (b) (chart speed, 60 cm/hr; flow rate, 1 ml/min; size of the peak fractions collected, 0.2 ml).

TABLE 1

RESIDUES IN CONTACT WITH F_{ab} FRAGMENTS 5B2 AND 10B7

VP2 Domain	VP3 Domain	VP3 Domain (cont.)
Leu 32	Lys 17	Arg 29
Ser 33	Leu 18	Arg 30
Lys 34[a]	Thr 19	Met 31
Ala 35	Phe 20	Ala 41
Met 36	Pro 21	Thr 42
Gly 38	Gln 22	Thr 153
Gly 39	Gly 23	Gly 154
Ser 154	Val 24[a]	Gly 158
Gly 155	Thr 25[a]	Asp 159
Pro 160	Ser 26	Leu 186
Thr 161	Glu 27	Leu 187
Thr 162	Val 28	
Asp 163		

[a] These residues (highlighted in Fig. 9) are spatially equivalent to the residues that define site 3B of poliovirus as determined by escape mutation analysis (Page *et al.*, 1988).

others are partially covered (Table 1). Because these residues are located on two different L subunits, the binding site spans a subunit interface.

DISCUSSION

Polyclonal and monoclonal antibodies are widely used in plant virology for identification and classification purposes, but this report is the first description of the tertiary structure of an icosahedral plant virus epitope. Escape mutation analysis is the most widely used technique by which animal virus epitopes are identified. This procedure cannot readily be applied to plant viruses because of the difficulty in establishing neutralization by antibodies in plants. Tremaine *et al.* (1986) examined the antigenic surface of southern bean mosaic virus with a panel of monoclonal antibodies; they identified regions of overlap and determined the number of binding sites per particle, but it was impossible to determine the F_{ab} footprints. The physical mapping described here has identified one site on the surface of CPMV that is common to two monoclonal antibodies. The procedure used selects for those antibodies with the strongest binding in solution and on the microscope grid. The common binding site we identified permits all 60 equivalent positions on the viral surface to be occupied with no overlap of symmetry equivalent F_{ab} fragments and this may be important for their detection by this procedure.

The binding site is formed at the interface of two L subunits. The covered regions correspond to portions of the VP2 and VP3 domains of picornaviruses (Fig. 1). Thus, the capsid quaternary structure is required for the formation of this site and this explains why 5B2 and 10B7 react only in sandwich type ELISAs. The antigenic surface of another comovirus, bean pod mottle virus, has been investigated with the synthetic peptide approach (Joisson *et al.*, 1993). This analysis revealed a site corresponding to NIm-IA in rhinovirus (see below), but was sensitive only to the portion of the 5B2 site on CPMV that lies on the VP2 domain (the peptide generating reactive antibodies contained residues 31–42 of the bean pod mottle virus VP2 domain).

Lys34 (VP2 domain) and Thr25 (VP3 domain), the most prominent residues within the F_{ab} footprint on CPMV, are spatially equivalent to the corresponding amino acids that define the 3B antigenic site on poliovirus (Page *et al.*, 1988; Mosser *et al.*, 1989). If either of these two residues are changed to a different amino acid in poliovirus, the virus is no longer neutralized by a particular group of monoclonal antibodies. Analysis of this site in poliovirus has shown that it is dependent on assembly of multiple 14S subunits made up of a pentamer of the capsid polypeptides (Rombaut *et al.*, 1990). This result is consistent with the nature of the site determined in CPMV.

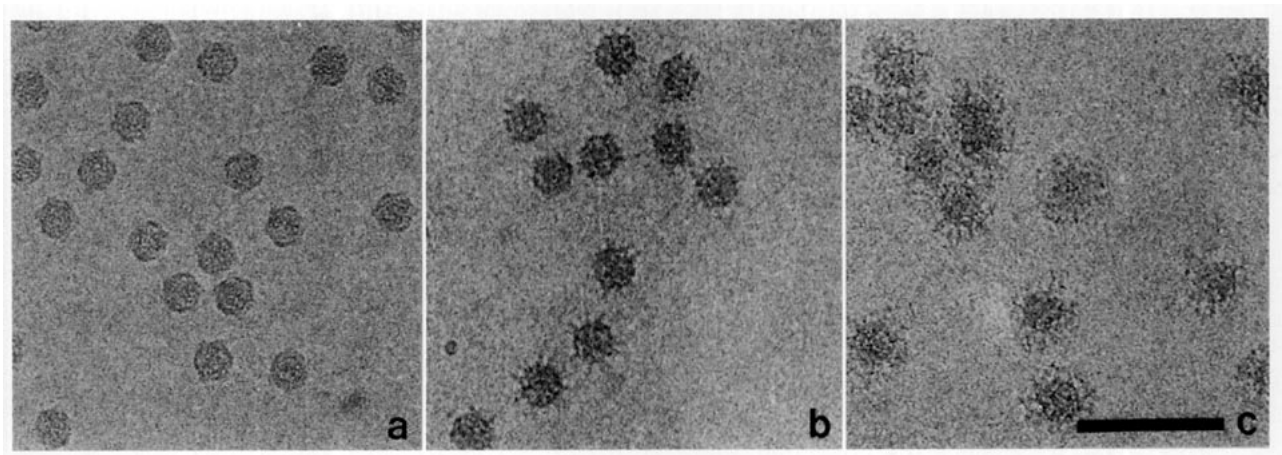

FIG. 6. CryoEM images of native CPMV (a), CPMV complexed with F_{ab} from antibody 5B2 (b), and CPMV complexed with IgG-5B2 (c). All micrographs were taken at a magnification of 49,000 and at a lens defocus of ~0.8 μm. The bar is 100 nm.

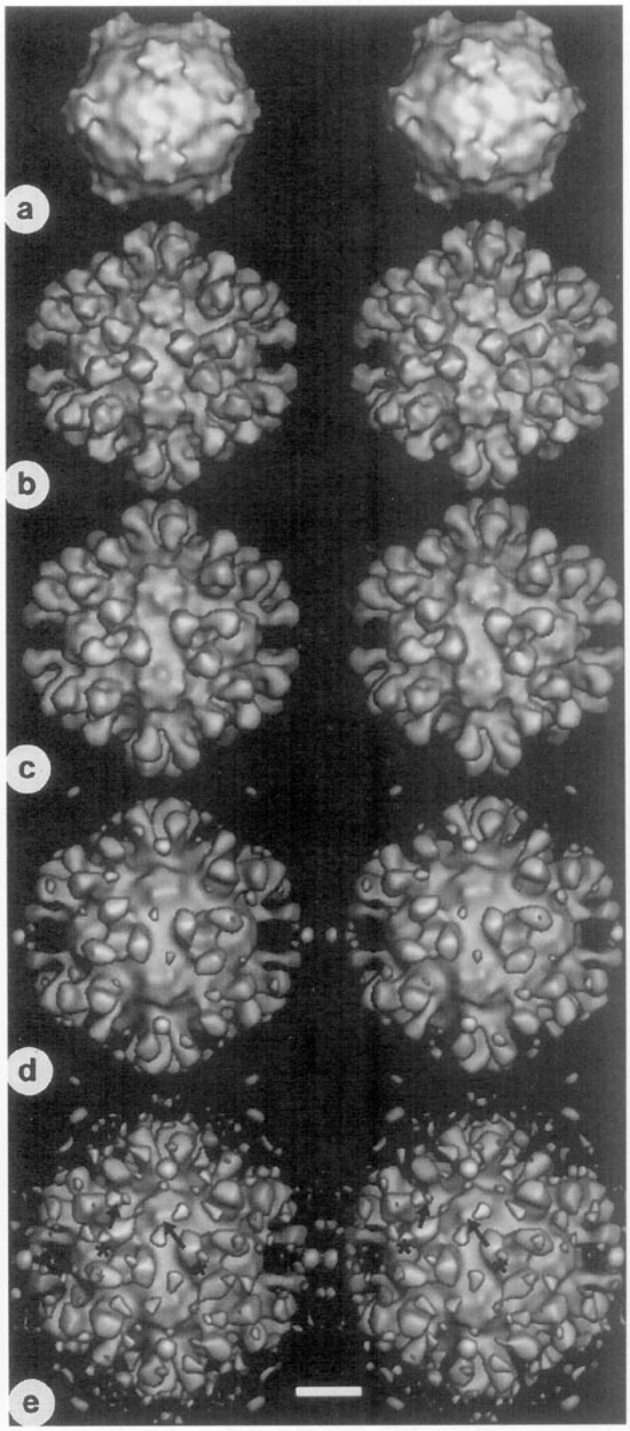

FIG. 7. A gallery of stereo images of reconstructed densities of native CPMV and CPMV complexed with F_{ab} fragments or IgG. The reconstructions with F_{ab} fragments are at ~23 Å resolution and the reconstruction with IgG is at 30 Å resolution. From top to bottom: (a) Native CPMV reconstructed from 17 particles. (b) CPMV complexed with F_{ab} from antibody 10B7 reconstructed from 27 particles. (c) CPMV complexed with F_{ab} from antibody 5B2 reconstructed from 23 particles. (d) CPMV complexed with IgG from McAb 5B2 reconstructed from 10 particles. This is contoured at a higher level than the reconstructions shown above to emphasize the F_{ab} density. (e) The bottom reconstruction is the same as immediately above, but contoured at the same level as the first three reconstructions. Figure 6c shows part of the micrograph used for the reconstruction and the higher density surrounding the particle is apparent. The strong density features that appear as "islands" are probably preferred positions for unbound F_{ab}. The arrow indicates the connection to the bound F_{ab} and the asterick indicates the F_c position. The bar is 5 nm.

Human rhinovirus 14 (HRV14) and poliovirus share a number of geometrically equivalent antigenic sites as determined by escape mutations. However, neutralizing immunogenic site III (NIm-III), the site on HRV14 that most closely corresponds to the 3B site of poliovirus, is confined to a single subunit, VP3 (Mosser *et al.*, 1989). The VP3 domain of the CPMV large subunit constitutes roughly two-thirds of the footprint for the 5B2 and 10B7 antibodies, thus this binding site is probably similar for HRV14 as well as for poliovirus.

The NIm-IA site on HRV14 has been analyzed by Smith *et al.* (1993a) with F_{ab} derived from McAb 17 using the same procedure reported here. This site differs in two ways from the 3B site discussed above. The F_{ab} 17 binding site is on subunit VP1 and all the regions of interaction between this F_{ab} and the virus are confined to a single subunit. In a subsequent report Smith *et al.* (1993b) have shown that the McAb 17 IgG binds in a bidentate fashion that maintains the icosahedral twofold symmetry. The distance between the centers of gravity of the twofold-related NIm-IA footprints is 110 Å. This is much longer than the corresponding distance between the twofold-related footprints in CPMV which is 78 Å. Although the 5B2 sites on CPMV are situated adjacent to twofold symmetry axes, there is no density connecting the twofold-related F_{ab} units. Each binding site must therefore correspond to an IgG with one F_{ab} attached and the other unattached. Mosser *et al.* (1989) considered the likelihood of bidentate binding for all the monoclonal antibodies that they analyzed for poliovirus and rhinovirus. They concluded that monoclonal antibodies binding to site 3B could not form a twofold axis-related bidentate interaction with the virus because the distance between these binding sites was less than 90 Å, the minimal distance estimated for bridging by an IgG (e.g., Icenogle *et al.*, 1983). The monodentate binding that we observed with the IgG of 5B2 supports this conclusion.

The cryoEM reconstruction of the IgG/CPMV structure contained islands of density that did not appear in either of the two different F_{ab}/CPMV reconstructions when all three were contoured at comparable levels. The lack of continuity in this additional density reflects the high mobility of the nonbound portions of the IgG. It was examined, however, to see if it might be consistent with marginally preferred positions of the Fc and nonbound F_{ab} portions of the IgG. To test this hypothesis we assumed that the relative positions of the F_{ab} units in an IgG would remain approximately the same in the bound and unbound states. We used the bidentate McAb 17 (Smith *et*

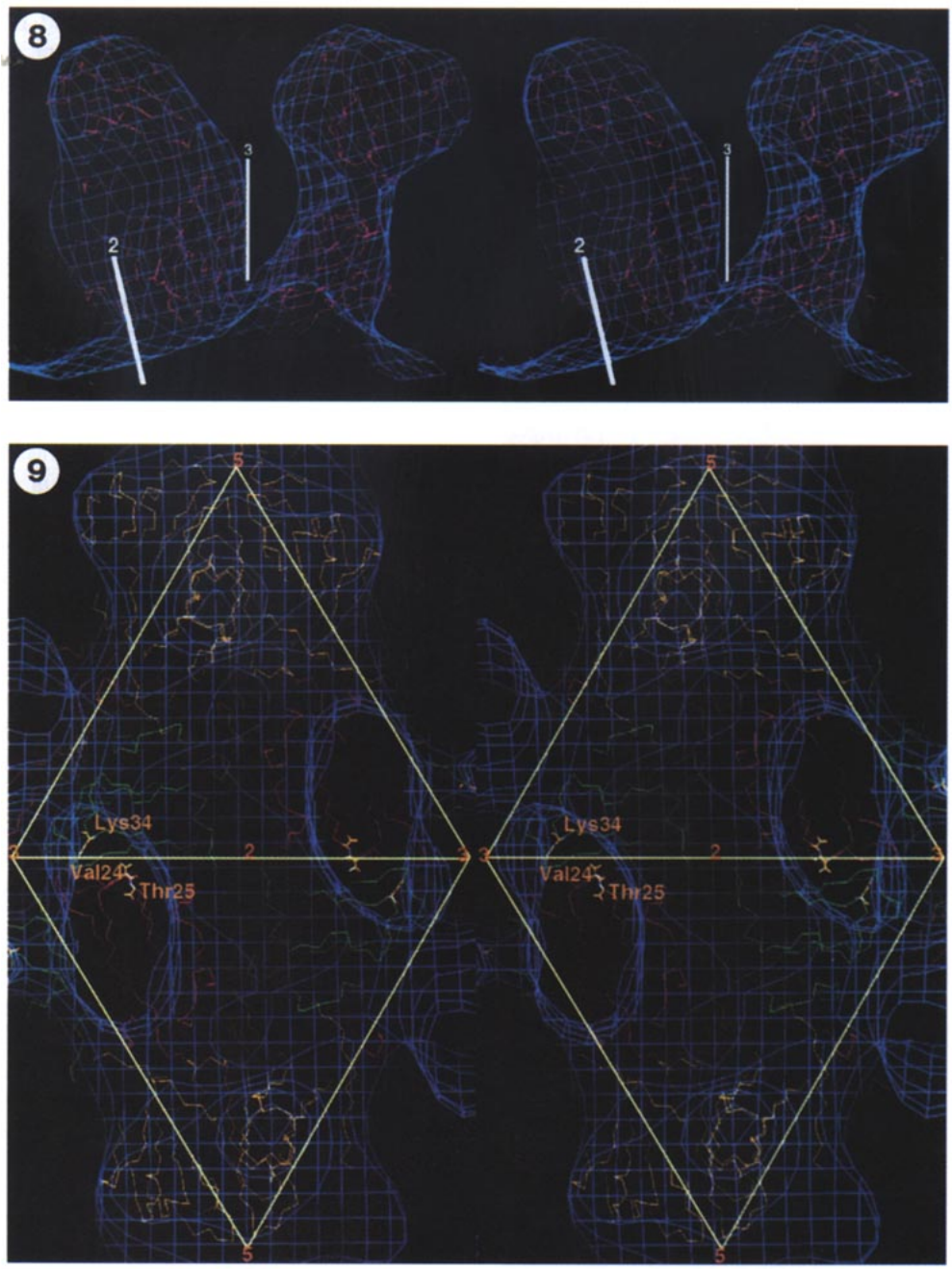

FIG. 8. Stereoview of density derived from the reconstruction of CPMV complexed with F_{ab} 10B7 shown in Fig. 7 compared with the atomic model of F_{ab} Kol used as a generic model for the F_{ab}.

FIG. 9. Stereoview of a detailed footprint of the F_{ab} on the surface of CPMV showing the residues in contact with F_{ab} 10B7. Lys 34 (VP2), Val 24 (VP3), and Thr 25 (VP3) are highlited in the Cα backbone. The electron density of the cryoEM reconstruction is shown as blue contours, the VP2 domain is shown in green, the VP3 domain is shown in red, and VP1 (small subunit) is shown in yellow.

al., 1993b) as a model to fit the IgG/CPMV density. The McAb17 model approximately fits the IgG-5B2 density in two orientations that are related by the pseudo twofold symmetry between the heavy and light chains of the F_{ab}. One orientation placed the unbound F_{ab} close to the threefold symmetry axes in severe steric overlap with threefold symmetry-related unbound F_{ab} fragments and away from the island of density. The other orientation placed the unbound F_{ab} in the center of gravity of the island density and in a sterically favorable location relative to symmetry-related, unbound F_{ab} units. In addition, a small piece of disconnected density was found in the position expected for the Fc. The possible preferred orientation of the unbound F_{ab} and the position for the Fc are depicted in Fig. 7.

By superimposing the McAb 17 coordinates to the IgG

5B2 complexes with CPMV density two further conclusions can be drawn. First, the F_{ab} elbow angles in both McAb17 and McAb 5B2 are similar, and second, the relative positions of the 5B2 F_{ab} heavy and light chains on the footprint are defined (the heavy variable domain lies primarily on the VP3 region of the CPMV subunits and the light variable domain lies primarily on the VP2 region). The former was already established by comparing the optimal F_{ab} models available which were used to fit the density in the two structures, while the latter was a consequence of the detailed analysis performed by Smith *et al.* (1993a) in which the orientation of the F_{ab} on the viral surface was established with the high resolution structure of McAb 17 F_{ab} (Liu *et al.,* 1994).

Knowledge of the antigenic sites on the surface of plant viruses has significance at two levels. First, epitopes might be classified as "natural" or "acquired" by comparing their character and location on related plant and animal viruses. Since plant viruses are not under the surveillance of a circulating immune system, the site common to 5B2 and 10B7 on comoviruses and 3B on poliovirus may result from quaternary structure that is shared by all viruses with a picorna-type capsid. In contrast, the NIm-1A site on rhinovirus appears to have evolved specifically for the purpose of "decoying" the immune system. This site and others consist of surface loops that are readily mutable without affecting other functions of the capsid structure. A second level of importance relates to the possible use of plant viruses as "expression systems" for animal virus epitopes through the genetic engineering of chimeric plant viruses that contain regions of polypeptide chains known to be antigenic on the surface of the animal virus (e.g., Usha *et al.,* 1993). The knowledge of naturally occurring antigenic sites on the surface of plant viruses may assist in making the most rational constructs or altering acquired immunity that may have resulted from previous exposure of an animal to a natural version of the virus. In CPMV, for instance, changing Lys34 or Thr35 in the 5B2 footprint may reduce natural immunity to native or altered CPMV particles.

The structures reported illustrate the power of combining the moderate resolution of cryoEM reconstructions of a complex with the high resolution structures of the components of the complex determined by X-ray crystallography. Although the actual resolution of the reconstruction is ~23 Å, the effective resolution with the combined information is much higher, because the atomic resolution structures of the components are known and can accurately be docked within the EM density. A shift of the F_{ab} fragment by as little as 5 Å significantly reduces the quality of the fit of the atomic model to the cryoEM density (Liu *et al.,* 1994). The footprint of the F_{ab} on the viral surface is defined with even greater precision than the overall fit of the F_{ab} model to the density, leaving virtually no doubt regarding which residues of the virus are covered by the F_{ab}. The combination of cryoEM and X-ray methods presented here is analogous to the refinement of protein structures. Structural data for typical proteins are available to only 2.5 Å but it is possible to refine these structures to within a fraction of an angstrom because the detailed structures of amino acids and small polypeptides are known and these dramatically constrain the stereochemistry of the protein. Similarly, the known high resolution structures of the components (the F_{ab} fragment and the virus) dramatically constrain the interpretation of the cryoEM reconstructions.

ACKNOWLEDGMENTS

We thank Tom Smith for providing us with the McAB17 coordinates and for helpful discussions, Professor Marc vanRegenmortel at the IBMC, Strasbourg, France, for his help with preparing the monoclonal antibodies and his continued support, and Sharon Fateley for help in preparing the manuscript. This work was supported by grants from the Public Health Service (AI18764) to J.E.J., the National Science Foundation (MCB9206305) to T.S.B., and a grant from the Lucille P. Markey Foundation for the development of structural biology at Purdue.

REFERENCES

Akerström, B., and Björck, L. (1986). A physiochemical study of protein G, a molecule with unique immunoglobulin G-binding properties. *J. Biol. Chem.* **261,** 10240–10247.

Amit, A. G., Mariuzza, R. A., Phillips, S. E. V., and Poljak, R. J. (1986). Three-dimensional structure of an antigen-antibody complex at 2.8 Å resolution. *Science* **233,** 747–753.

Attassi, M. Z., and Kurisaki, J. I. (1984). A novel approach for localization of the continuous protein antigenic sites by comprehensive synthetic surface scanning: Antibody and T-cell activity to several influenza hemagglutinin synthetic sites. *Immunol. Commun.* **13,** 539–551.

Baker, T. S., Drak, J., and Bina, M. (1988). Reconstruction of the three-dimensional structure of simian virus 40 and visualization of the chromatin core. *Proc. Natl. Acad. Sci. USA* **85,** 422–426.

Baker, T. S., Newcomb, W. W., Olson, N. H., Cowsert, L. M., Olson, C., and Brown, J. C. (1991). Structures of bovine and human papillomaviruses. Analysis by cryoelectron microscopy and three-dimensional reconstruction. *Biophys. J.* **60,** 1445–1456.

Brunger, A. T. (1988). Crystallographic refinement by simulated annealing application to a 2.8 Å resolution structure of aspartate aminotransferase. *J. Mol. Biol.* **203,** 803–816.

Chen, Z., Stauffacher, C. V., and Johnson, J. E. (1990). Capsid structure and RNA packaging in comoviruses. *Sem. Virol.* **1,** 453–466.

Chen, Z., Stauffacher, C., Li, Y., Schmidt, T., Bomu, W., Kamer, G., Shanks, M., Lomonossoff, G. P., and Johnson, J. E. (1989). Protein–RNA interactions in an icosahedral virus at 3.0 Å resolution. *Science* **245,** 154–159.

Cheng, R. H., Olson, N. H., and Baker, T. S. (1992). Cauliflower mosaic virus: A 420 subunit ($T = 7$), multilayer structure. *Virology* **186,** 655–668.

Chow, M., Yabrov, R., Bittle, J., Hogle, J., and Baltimore, D. (1985). Synthetic peptides from four separate regions of the poliovirus type 1 capsid protein VP1 induce neutralization antibodies. *Proc. Natl. Acad. Sci. USA* **82,** 910–914.

Colman, P. M., Laver, W. G., Varghese, J. N., Baker, A. T., Tulloch, P. A., Air, G. M., and Webster, R. G. (1987). Three-dimensional structure of a complex of antibody with influenza virus neuraminidase. *Nature* **326,** 358–363.

COULTER, A., and HARRIS, R. (1983). Simplified preparation of rabbit F_{ab} fragments. *J. Immunol. Methods* **59,** 199–203.

DORE, I., WEISS, E., ALTSCHUH, D., and VAN REGENMORTEL, M. H. V. (1988). Visualization by electron microscopy of the location of tobacco mosaic virus epitopes reacting with monoclonal antibodies in enzyme immunoassay. *Virology* **162,** 279–289.

DRYDEN, K. A., WANG, G., YEAGER, M., NIBERT, M. L., COOMBS, K. M., FURLONG, D. B., FIELDS, B. N., and BAKER, T. S. (1993). Early steps in reovirus infection are associated with dramatic changes in supramolecular structure and protein conformation: Analysis of virions and subviral particles by cryoelectron microscopy and image reconstruction. *J. Cell. Biol.* **122,** 1023–1041.

FAZEKAS DE ST. GROTH, S., and SCHEIDEGGER, D. (1980). Production of monoclonal antibodies: Strategy and tactics. *J. Immunol. Methods* **35,** 1–21.

FULLER, S. D. (1987). The $T = 4$ envelope of sindbis virus is organized by interactions with a complementary $T = 3$ capsid. *Cell* **48,** 923–934.

HENDRICKSON, W. A. (1985). Stereochemically restrained refinement of macromolecular structures. *In* "Methods in Enzymology" (H. W. Wyckoff, C. H. S. Hirs, and S. N. Timashaff, Eds.), Vol. 115, pp. 252–270. Academic Press, San Diego.

HOGLE, J. M., CHOW, M., and FILMAN, D. J. (1985). Three-dimensional structure of poliovirus at 2.9 Å resolution. *Science* **229,** 1358–1365.

ICENOGLE, J., SHIWEN, H., DUKE, G., GILBERT, S., RUECKERT, R., and ANDEREGG, J. (1983). Neutralization of poliovirus by a monoclonal antibody: Kinetics and stoichiometry. *Virology* **127,** 412–425.

JOISSON, C., KUSTER, F., PLAUE, S., and VAN REGENMORTEL, M. (1993). Antigenic analysis of bean pod mottle virus using linear and cyclized synthetic peptides. *Arch. Virol.* **128,** 299–317.

LIU, H., SMITH, T. J., LEE, W.-M., MOSSER, A. G., RUECKERT, R. R., OLSON, N. H., CHENG, R. H., and BAKER, T. S. (1994). Structure determination of an F_{ab} fragment that neutralizes human rhinovirus 14 and analysis of the F_{ab}-virus complex. *J. Mol. Biol.* **240,** 127–137.

LOMONOSSOFF, G. P., and JOHNSON, J. E. (1991). The synthesis and structure of comovirus capsids. *Prog. Biophys. Molec. Biol.* **55,** 107–137.

MCCULLOUGH, K. C., CROWTHER, J. R., and BUTCHER, R. N. (1985). Alteration in antibody reactivity with foot-and-mouth disease virus (FMDV) 146 S antigen before and after binding to a solid phase or complexing with specific antibody. *J. Immunol. Methods* **82,** 91–100.

MCKINNEY, M. M., and PARKINSON, A. (1987). A simple, non-chromatographic procedure to purify immunoglobulins from serum and ascites fluid. *J. Immunol. Methods* **96,** 271–278.

MOSSER, A. G., LEIPPE, D. M., and RUECKERT, R. R. (1989). Neutralization of picornaviruses: Support for the pentamer bridging hypothesis. *In* "Molecular Aspects of Picornavirus Infection and Detection" (B. L. Semler and E. Ehrenfeld, Eds.), pp. 155–167. Amer. Soc. Microbiol., Washington, DC.

PADLAN, E. A., SILVERTON, E. W., SHERIFF, S., COHEN, G. H., SMITH-GILL, S. J., and DAVIES, D. R. (1989). Structure of an antibody–antigen complex: Crystal structure of the HyHEL–10 F_{ab}–lysozyme complex. *Proc. Natl. Acad. Sci. USA* **86,** 5938–5942.

PAGE, G. S., MOSSER, A. G., HOGLE, J. M., FILMAN, D. J., RUECKERT, R. R., and CHOW, M. (1988). Three-dimensional structure of poliovirus serotype 1 neutralizing determinants. *J. Virol.* **62,** 1781–1794.

REYNOLDS, C., PAGE, G., ZHOU, H., and CHOW, M. (1991). Identification of residues in VP2 that contribute to poliovirus neutralization antigenic site 3B. *Virology* **184,** 391–396.

ROMBAUT, B., BOEYE, A., FERGUSON, M., MINOR, P., MOSSER, A., and RUECKERT, R. (1990). Creation of an antigenic site in poliovirus type 1 by assembly of 14S subunits. *Virology* **174,** 305–307.

ROSSMANN, M. G., ARNOLD, E., ERICKSON, J. W., FRANKENBERGER, E. A., GRIFFITH, J. P., HECHT, H. J., JOHNSON, J. E., KAMER, G., LUO, M., MOSSER, A. G., RUECKERT, R. R., SHERRY, B., and VRIEND, G. (1985). Structure of a human common cold virus and functional relationship to other picornaviruses. *Nature* **317,** 145–153.

SHERRY, B., MOSSER, A. G., COLONNO, R. J., and RUECKERT, R. R. (1986). Use of monoclonal antibodies to identify four neutralization immunogens on a common cold picornavirus, human rhinovirus 14. *J. Virol.* **57,** 246–257.

SMITH, T. J., OLSON, N. H., CHENG, R. H., LIU, H., CHASE, E. S., LEE, W. M., LEIPPE, D. M., MOSSER, A. G., RUECKERT, R. R., and BAKER, T. S. (1993a). Structure of human rhinovirus complexed with F_{ab} fragments from neutralizing antibody. *J. Virol.* **67,** 1148–1158.

SMITH, T. J., OLSON, N. H., CHENG, R. H., CHASE, E. S., and BAKER, T. S. (1993b). Structure of a human rhinovirus-bivalently bound antibody complex: implications for viral neutralization and antibody flexibility. *Proc. Natl. Acad. Sci. USA* **90,** 7015–7018.

STOCKER, J. W., FOSTER, H. K., MIGGIANO, V., STAHLI, C., STAIGER, G., TAKACS, B., and STAEHELIN, Th. (1982). Generation of two new myeloma cell lines "PAI" and "PAI-O" for hybridoma production. *Res. Discl.* **217,** 155–157.

TREMAINE, J. H., MACKENZIE, D. J., and RONALD, W. P. (1986). Determination of affinity constants and the number of binding sites of monoclonal antibodies specific for southern bean mosaic virus. *Virology* **155,** 452–459.

TRINICK, J., and COOPER, J. (1990). Concentration of solutes during preparation of aqueous suspensions for cryo-electron microscopy. *J. Microsc.* **159,** 215–222.

USHA, R., ROHLL, J. B., SPALL, V., SHANKS, M., MAULE, A. J., JOHNSON, J. E., and LOMONOSSOFF, G. P. (1993). Expression of an Animal Virus Antigenic Site on the Surface of a Plant Virus Particle. *Virology* **197,** 366–374.

WANG, G., PORTA, C., CHEN, Z., BAKER, T. S., and JOHNSON, J. E. (1992). Identification of a F_{ab} interaction site (footprint) on a spherical virus by cryo-electron microscopy and X-ray crystallography. *Nature* **355,** 275–278.

WHITE, J. M., and JOHNSON, J. E. (1980). Crystalline cowpea mosaic virus. *Virology* **101,** 319–324.

WILEY, D. C., WILSON, I. A., and SKEHEL, J. J. (1981). Structural identification of the antibody-binding sites of Hong Kong influenza haemagglutinin and their involvement in antigenic variation. *Nature (London)* **289,** 373–378.

WILSON, I. A., and COX, N. J. (1990). Structural basis of immune recognition of influenza virus hemagglutinin. *Annu. Rev. Immunol.* **8,** 737–771.

WINKELMANN, D. A., BAKER, T. S., and RAYMENT, I. (1991). Three-dimensional structure of myosin subfragment-1 from electron microscopy of sectioned crystals. *J. Cell Biol.* **114,** 701–713.